SYNTHESIS AND CHARACTERISATION OF TITANIUM DIOXIDE NANOPARTICLES (TiO_2 NPs) FROM HEAVY MINERAL SAND

Aung Thura[1], Hla Naning[2], Htet Ko Ko[3], Aung Myo Thu[4], Phyo Wai Zaw[5], Pyae Phyo Aung[6]

Abstract

This research work concerns the synthesis and characterisation of titanium dioxide nanoparticles (TiO_2 NPs) from heavy mineral sand (HMS). In this research work HMS was collected from the Moemeik Myitsone area and analysed for elemental and mineralogical compositions. A physical beneficiation process (gravity separation and magnetic separation) was performed for the enrichment of ilmenite from collected HMS and characterised by XRD, ED-XRF, and SEM analyses. After the physical beneficiation process, a chemical treatment process (alkali digestion known as) was carried out with the variation of operating parameters for the synthesis of titanium dioxide nanoparticles (TiO_2 NPs) from ilmenite concentrate. Alkali digestion products and synthesised TiO_2 NPs were also characterised by XRD, ED-XRF, and SEM analyses. The optimal operating parameters for alkali digestion and iron removal efficiencies for the synthesis of TiO_2 NPs from HMS have been examined in accordance with the related experimental results. Ti is enriched to 30.18% in the eleminte countate. 22.33 % of Iron in the elemite is also removed by this frocess.

Keywords: heavy mineral sand, physical beneficiation, chemical treatment, ilmenite concentrate, digestion product, titanium dioxide nanoparticles

Introduction

Nanotechnology has become one of the most popular topics in the recent decade as it evolves into becoming a key technology in the 21st century (Shilpy Bhullar et al., 2021). Generally, nanotechnology can be defined as the creation of nanoparticles with a dimension ranging from 1 to 100 nm by manipulating the atomic and molecular matter through new techniques or devices (Ajamaluddin Malik et al., 2021). TiO_2 is the most astounding nanomaterial because of its chemical stability, photocatalytic properties, high stability, biocompatibility, and non-toxicity (Seman N et al., 2022).

Titanium is a very important element for several industrial applications, being one of the ninth most abundant elements in the Earth's crust (Iqbal Firdaus et al., 2021). HMS deposits are the main source of titanium feedstock for the titanium dioxide (TiO_2) pigments industry, obtained from the minerals ilmenite, rutile and leucoxene. HMS deposits are also the principal source of zircon ($ZrSiO_4$), from which zirconium dioxide (ZrO_2) is obtained for uses mostly in refractory products. Sometimes monazite [$(Ce, La, Nd,Th)PO_4$] is recovered as a byproduct mineral, sought for its rare earth elements, and thorium (Bradley S. Van Gosen et al., 2016).

There are various techniques that can be adopted for the preparation of TiO_2 NPs such as the sol-gel method, instantaneous synthesis method, solvothermal method, microwave-assisted synthesis, simple mixing, and precipitation method (Seman N et al., 2022). In the current research work, the simple mixing and precipitation method was used to synthesise TiO_2 NPs because it does not require any complicated process and complex preparation conditions in addition to its usefulness and attractiveness that can easily control the particles' size and shapes.

[1] Faculty of Chemistry, Defence Services Academy, Pyin Oo Lwin
[2] Faculty of Chemistry, Defence Services Academy, Pyin Oo Lwin
[3] Faculty of Chemistry, Defence Services Academy, Pyin Oo Lwin
[4] Faculty of Chemistry, Defence Services Academy, Pyin Oo Lwin
[5] Faculty of Chemistry, Defence Services Academy, Pyin Oo Lwin
[6] Faculty of Chemistry, Defence Services Academy, Pyin Oo Lwin

Aim

The aim of research work is to synthesise and characterise titanium dioxide nanoparticles (TiO_2 NPs) from heavy mineral sand.

Materials and Methods

The principal materials and methods which play an important role in the production of titanium oxide nanoparticles (TiO_2 NPs) are expressed in this section.

Sample Collection and Preparation

The HMS used in this study was collected from the confluence site of the Shweli River and Nammeik Creek in the Myitsone area of Moemeik Township, Northern Shan State. The collected HMS was repeatedly washed with water to remove clay, silt, and other impurities and then dried, weighed, and analysed by XRD and ED-XRF. For physical beneficiation, the collected HMS was ground until the products passed through a 100 mesh size sieve. Figure 1 shows *(a)* the collected raw HMS and *(b)* ground HMS.

Figure 1. (a) Raw heavy mineral sand and (b) ground heavy mineral sand

Physical Beneficiation of HMS

The ground HMS was initially concentrated by a gravity separation process. The heavy mineral concentrate (HMC) separated by the table shaking process dried in sunlight for the next process of magnetic separation. The HMC was then secondly separated by using a magnetic separator into non-magnetic minerals, low-magnetic minerals and magnetic titanium-bearing minerals for desired paramagnetic titanium-bearing minerals ($FeTiO_3$). The ilmenite concentrate received after the magnetic separation process was analysed by XRD and ED-XRF.

Alkali Digestion of Ilmenite Concentrate

After physical beneficiation, ilmenite concentrate was then ground and sieved until the required mesh size of -150 because a potent oxidant and a lengthy retention period are needed to oxidize the ferrous minerals during alkali digestion.

By using the stainless steel bladed overhead stirrer, each experiment was carried out in a 400 ml thermal-resistant glass beaker and stainless steel beaker (SUS316) with an appropriate lid intended to prevent evaporation and a sand bath for stable temperature control on the electric ceramic stove at 220°C. The process of alkali digestion is expressed in Figure. 2:

Figure 2. Flow diagram of alkali digestion process

For each run, the beaker was first filled with a specific amount of solid KOH and the required amount of distilled water to get 72 wt. % of alkali solution. The beaker was then heated while being stirred continuously (400 rpm). A specific weighed amount of ilmenite was added to the beaker once the solution temperature reached the target level and remained constant. In this process, alkali digestions were performed by the variations of digestion times: 90, 120, 150, 180, 210, 240, 270, and 300 min, and ilmenite to alkali weight ratios of 1:3, 1:5, 1:7, and 1:9.

After the end of the specific digestion time, solid/liquid separation was performed into digestion product and residue. Filtration and washing were then accomplished with warm distilled water by using the vacuum pump until the pH reaches ~7, which was monitored by Cobra4 mobile-link2 with the sensor unit chemistry, and then dried for 24 hours at 140°C in the drying oven. After that, the dried digestion products were analysed by XRD, ED-XRF, and SEM.

Iron Removal from Digestion Product and Synthesis of TiO_2 NPs

To obtain leach liquor, the digestion product was leached in a 9 M HCl solution at 80°C, stirring speed of 900 rpm, and an operation time of 60 min by the magnetic stirrer. The liquid/solid mass ratio was adjusted to be 6. After acid leaching, the leachate solution was cooled at room temperature, and then a certain amount of EDTA disodium salt was dissolved in the leachate solution to act as the chelating agent for Fe ions and prevent the formation of $Fe(OH)_3$/$Fe(OH)_2$. Fe(III) ion forms a complex ion with EDTA according to the following balanced equation:

$$Fe^{3+} + EDTA \rightleftharpoons Fe(EDTA)^{3+} \quad (1)$$

The iron removal and synthesis of TiO_2 NPs process is shown in Figure. 3.

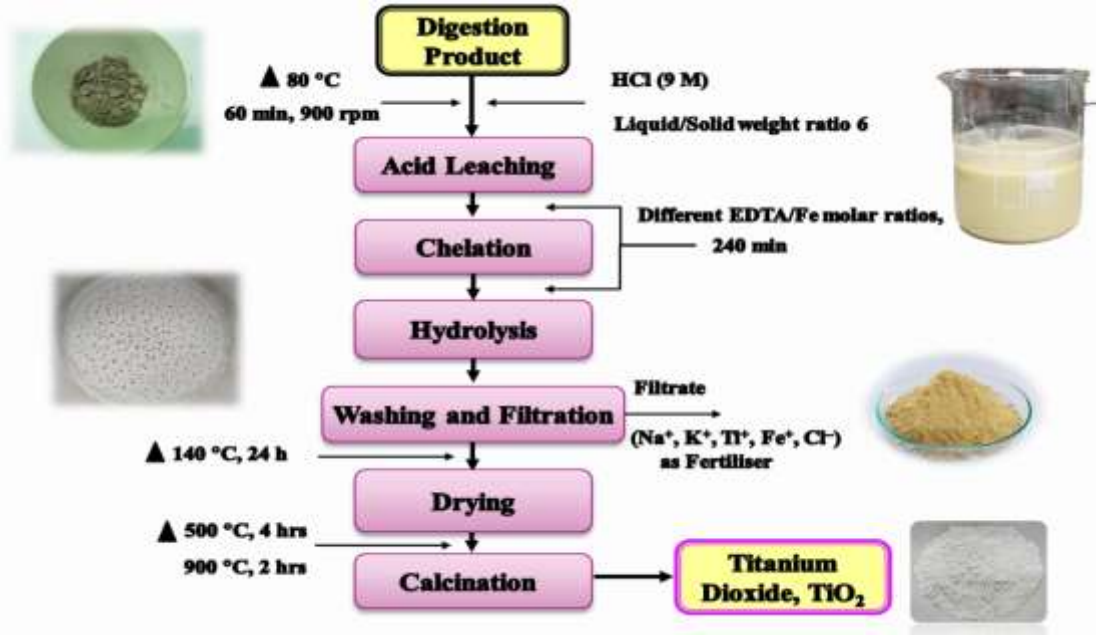

Figure 3. Flow diagram for the removal of iron from digestion product

For each test to achieve certain molar ratios of EDTA/Fe (3:1, 3.5:1, 4:1, 4.5:1, 5:1, 6:1, 8:1, and 10:1), the amount of EDTA was adjusted by gravimetric means. The acidity of the solution (pH~2) was controlled by adding the KOH solution. Hydrolysis of the solution proceeded for 4 hours with vigorous stirring at room temperature. After that, the slurry was filtered out by using a vacuum pump, and the precipitates were washed with warm distilled water and dried at 140°C for 24 hours. The dried precipitates were then calcined in the muffle furnace at 500°C for 4 hours and 900°C for 2 hours to get the appropriate crystal phase of TiO_2. The by-products, filtrates containing Fe(III)-EDTA complexes and some other constituents, were separately stored and dried them at 100 ℃ for the elimination of water. The calcined TiO_2 powders were analysed by XRD, ED-XRF, and SEM.

Results and Discussion

Characterisation of Collected HMS and Ilmenite Concentrate

The XRD spectra of Moemeik Myitsone HM sand and ilmenite concentrate are shown in Figures 4 (a) and (b).

The mineralogical analysis of the Moemeik Myitsone HMS reveals the presence of five minerals, ilmenite ($FeTiO_3$), rutile (TiO_2), monazite ($CePO_4$), zircon ($ZrSiO_4$), and cassiterite (SnO_2). Only ilmenite and rutile are the minerals that contain titanium; the other three do not. By the X-ray Diffraction Spectrum of ilmenite concentrate, ilmenite comprises the main portion in the physically enriched ilmenite concentrate. Other compounds may also comprise a trace amount of it. This improves the alkali digestion, the following step in the separation process, to be more advantageous. On the other hand, non-magnetic heavy minerals such as monazite, zircon, and cassiterite are concentrated as by-products.

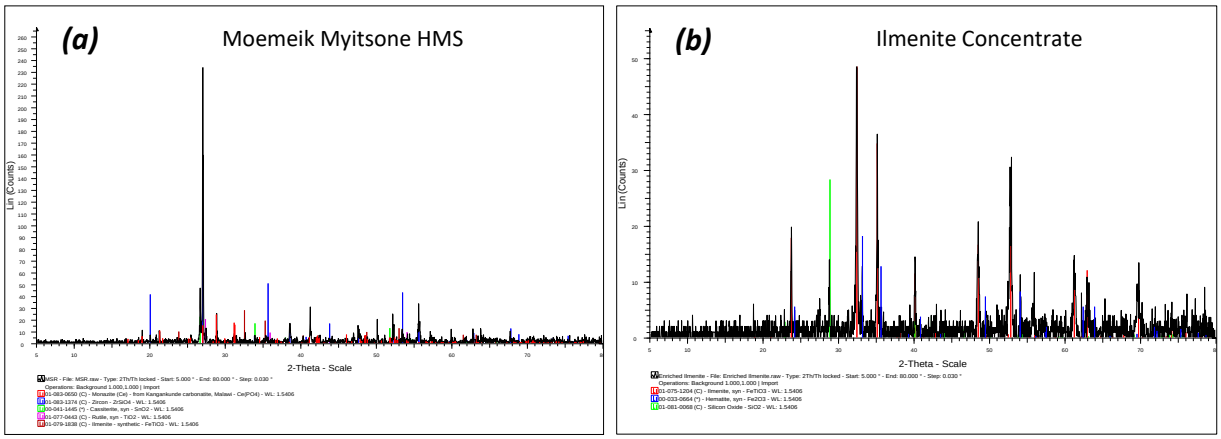

Figure 4. XRD spectra of ***(a)*** moemeik myitsone hms and ***(b)*** ilmenite concentrate

Table 1. Comparison of Elemental Compositions in HMS and Ilmenite Concentrate

No.	Elements	Z	Content in HMS (%)	Content in Ilmenite Concentrate (%)
1	Mg	12	0.129	0.691
2	Al	13	0.580	2.371
3	Si	14	9.704	2.360
4	P	15	2.340	0.429
5	K	19	0.121	0.035
6	Ca	20	0.225	0.017
7	Ti	22	11.090	30.181
8	Mn	25	0.340	11.051
9	Fe	26	9.371	22.331
10	Y	39	0.319	0.037
11	Zr	40	9.122	0.107
12	Sn	50	3.002	0.010
13	La	57	1.340	0.341
14	Ce	58	4.160	0.612
15	Others		48.167	29.427

Table 1. indicates the comparison of elemental compositions in HMS and ilmenite concentrate. In this comparison, it can be seen that the percentage of titanium is increased significantly (nearly threefold), and that of iron is also increased nearly twofold by means of physical beneficiation. Therefore, the next step of the chemical treatment can be convenient.

Characterisation of Ilmenite Concentrate, Digestion Product, and Residue

Discernible peaks are not found in the XRD spectra (Figure 5, a), therefore the digestion products are roughly amorphous. Most of the XRD peaks of the residues correspond to $FeTiO_3$, Fe_2O_3, and SiO_2 (Figure 5, b). Though the digestion products are roughly amorphous, it can be

assumed that during the alkali digestion process, ilmenite concentrate is decomposed into potassium titanate ($K4Ti_3O_8$) and hematite (Fe_2O_3), and it would be confirmed by the SEM and this can be interpreted as the following reaction:

$$12FeTiO_3 + 16KOH + 3O_2 \rightarrow 4K_4Ti_3O_8 + 6Fe_2O_3 + 8H_2O \quad (2)$$

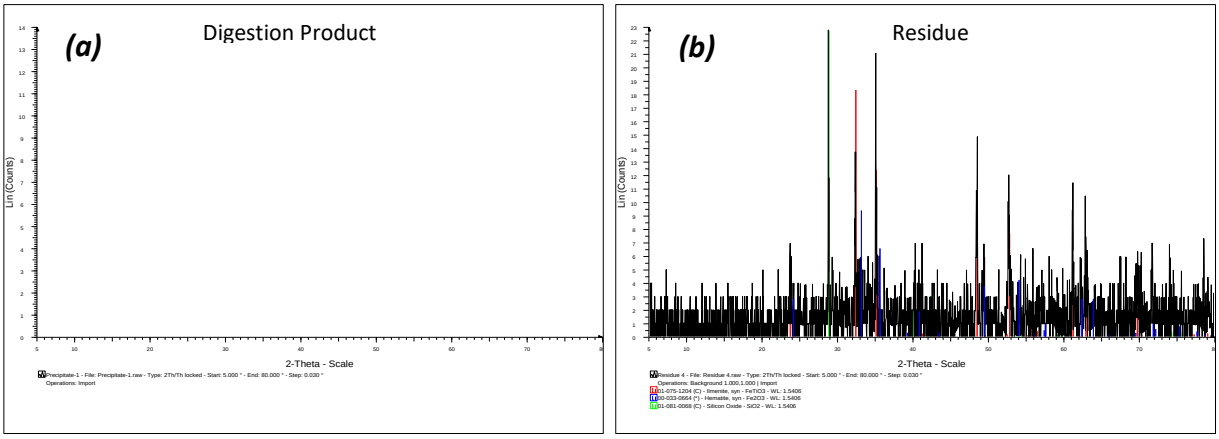

Figure 5. XRD spectra of *(a)* digestion product and *(b)* residue

The SEM analysis reveals the surface morphology of ilmenite concentrate and digestion product expressed in figures 6 (a) and (b), and the formation of masking on residue, along with the longer ilmenite-alkali digestion time established in figures 7 (a) and (b).

By looking at the surface morphology of ilmenite concentrate and digestion product, it can be seen that the structure of ilmenite concentrate has a crystalline appearance with mean particle length of 6 µm, and the structure of digestion product has a rod-like potassium titanate structure with a particle length of 4 µm on average.

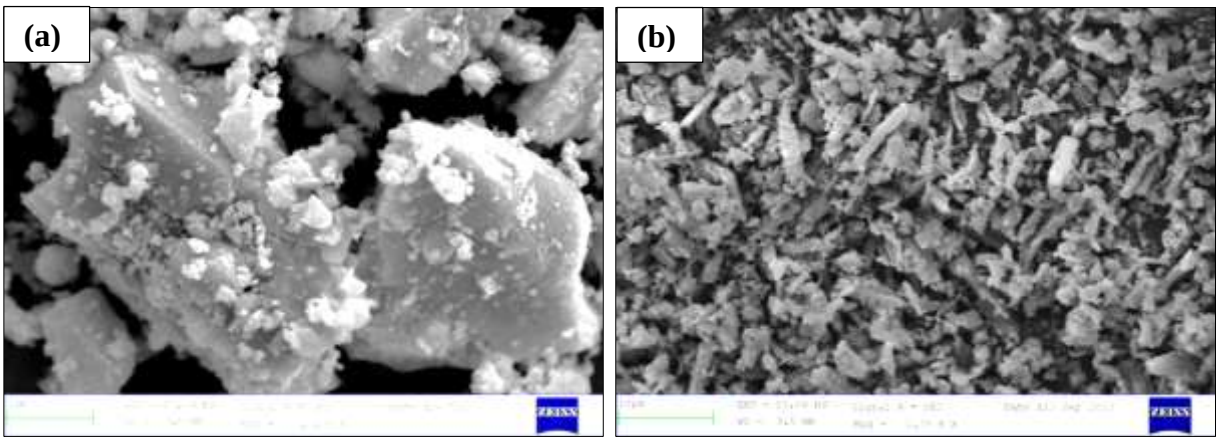

Figure 6. SEM micrographs of *(a)* ilmenite concentrate and *(b)* digestion product

In contrast to the ilmenite structure, in Figure 7 (a), it is also evident that the residual particles are grouped into spherical aggregates as big as 200 µm on average. It may be assumed that longer digestion time at high temperatures causes the masking on the outermost surface of ilmenite particles with potassium titanate ($K_4Ti_3O_8$, $K_2Ti_8O_{17}$, $K_2Ti_6O_{13}$), titanium oxy-hydroxide $TiO(OH)_2$, titanium dioxide TiO_2, titanium hydroxide $Ti(OH)_4$, iron oxide (Fe_2O_3, FeO) and so on. In this situation, ilmenite concentrate no longer reacts with the KOH and is unavailable to decompose because it is fully blocked by the masking. In Figure 7 (b), the SEM image of the rod-shaped potassium titanates and spherical iron oxides blocked on ilmenite particles is magnified. As demonstrated, potassium titanates particles have crystallised with a mean particle length of 15

μm and a mean particle width of 2 μm, and round iron oxide (FeO, Fe_2O_3 and Fe_3O_4) particles have formed with a diameter of roughly 0.5 μm.

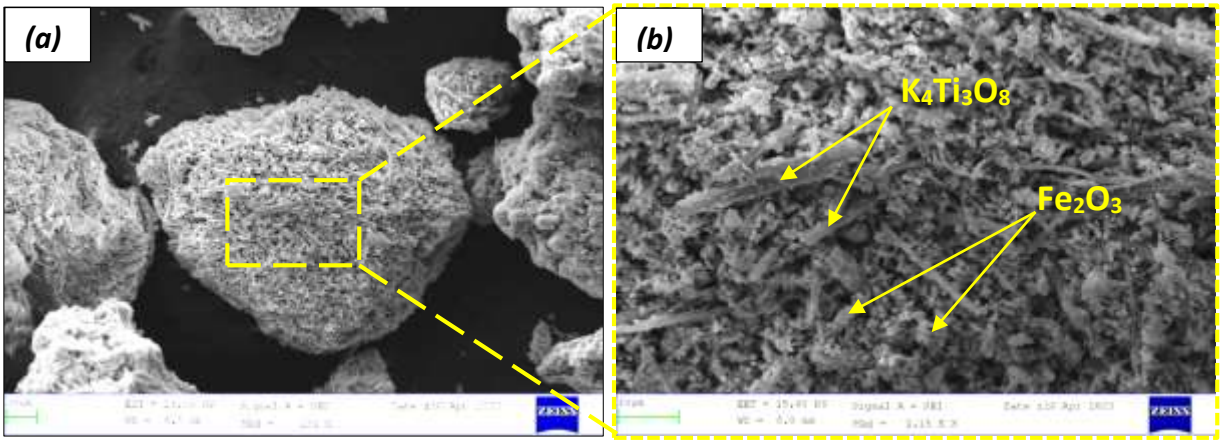

Figure 7. SEM micrographs of potassium titanate and iron oxide blocked on ilmenite

Comparison of Titanium Extraction Efficiencies in Different Containers

The extraction efficiencies of titanium performed by relative operating parameters with different containers are expressed in Figures 8 (a) and (b).

As the results described in Figure 8 (a) and Table 2, the extraction efficiency of titanium operated with steel beaker for digestion time 90 min is ~93 %, that for digestion time 120 min to 240 min increases up to ~98 to ~99 %, and that for digestion time 270 min and after noticeably decreases to ~84 %. Among these experiments, a digestion time of 120 min can be considered as the optimum for steel beaker since its Ti extraction efficiency is ~98 % and it saves time and more benefits compared to others longer digestion times.

And the extraction efficiency of titanium operated with a glass beaker for digestion time 90 min to 210 min increases steadily ~18 % to ~36 %, but that for digestion time 240 min to 300 min increases significantly ~70 % to ~81 %. In these processes, digestion time of 240 min is determined as the optimum for glass beaker because washing time is more favourable compared to longer digestion times. Accordingly, highly distinctive extraction efficiencies of titanium are observed in this comparison of titanium extraction efficiencies in different containers with relative digestion times.

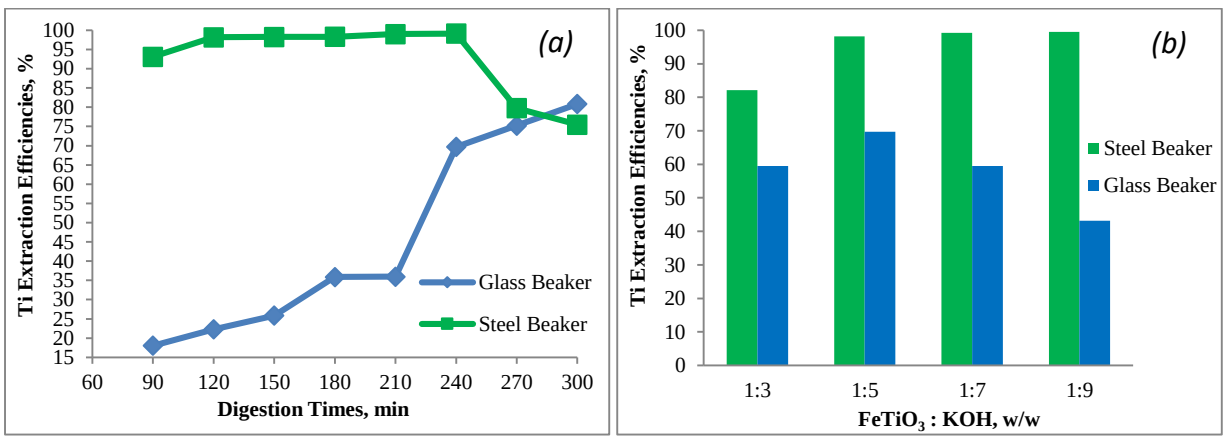

Figure 8. Titanium extraction efficiencies operated in different containers with relative (a) digestion times and (b) ilmenite to alkali weight ratio

The data described in Figure 8 (b) and Table 3 show the titanium extraction efficiencies in different containers with relative ilmenite to alkali weight ratios. By the experimental data that

result from the operation with steel beaker and different ilmenite to alkali weight ratios, titanium extraction efficiency of ilmenite to alkali weight ratio 1:3 is ~82 % and that of ilmenite to alkali weight ratios of 1:5 to 1:9 picks up ~98 % to 99.5 %, respectively.

In contrast to the titanium extraction efficiencies resulting from the operation with a steel beaker, the extraction efficiencies of titanium performed by a glass beaker and different ilmenite to alkali weight ratios decrease continuously following the ilmenite to alkali weight ratio of 1:5. As the results, ilmenite to alkali weight ratio of 1:5 is observed as the optimum for both containers.

Table 2. Effect of Digestion Time on Titanium Extractions in Different Containers

Time (min)			Extracted Ti (Glass Beaker)		Extracted Ti (Steel Beaker)	
Digestion	Washing until ~pH7		Content (g)	Extraction (%)	Content (g)	Extraction (%)
	Glass	Steel				
90	300	300	1.090	18.06	5.619	93.096
120	300	300	1.346	22.30	5.926	**98.180**
150	300	300	1.561	25.86	5.930	98.236
180	300	300	2.165	35.87	5.933	98.301
210	300	300	2.171	35.97	5.977	99.015
240	300	300	4.206	69.68	5.983	99.124
270	840	300	4.539	75.20	4.814	79.751
300	2160	300	4.878	80.82	4.556	75.488
Ti = 6.036 g and Fe = 4.466 g in Ilmenite Concentrate						

Table 3. Effect of Ilmenite to Alkali Weight Ratio on Titanium Extractions performed with Related Optimal Digestion Times in Different Containers

$FeTiO_3$: KOH, w/w	Time (min)				Extracted Ti (Glass Beaker)		Extracted Ti (Steel Beaker)	
	Digestion		Washing until ~pH7		Content (g)	Extraction (%)	Content (g)	Extraction (%)
	Glass	Steel	Glass	Steel				
1:3	240	120	300	300	3.593	59.52	4.957	82.131
1:5	**240**	**120**	**300**	**300**	**4.210**	**69.75**	**5.926**	**98.180**
1:7	240	120	480	480	3.590	59.48	5.992	99.274
1:9	240	120	570	570	2.604	43.14	6.006	99.499
Ti = 6.036 g and Fe = 4.466 g in Ilmenite Concentrate								

By the comparison of the titanium extraction efficiencies performed by the different containers with relative digestion times and ilmenite to alkali weight ratios, the extraction efficiency of titanium operated with a steel beaker with a digestion time of 120 min and ilmenite to alkali weight ratio of 1:5 is much higher than that operated with a glass beaker.

Comparison of Metal Extraction Efficiencies in Different Containers with Related Optimal Operating Parameters

According to the experimental data that is described in Table 4, titanium is extracted ~4 g from the total 6.036 g of titanium in ilmenite concentrate by the digestion with a glass container for optimum digestion time of 240 min and ilmenite to alkali weight ratio of 1:5. Titanium extraction by alkali digestion operated in a steel container with an optimum digestion time of 120 min and an ilmenite to alkali weight ratio of 1:5 increases and nearly fully recovers ~6 g from the total 6.036 g of titanium in the ilmenite concentrate, but iron content is slightly higher than that in the original content in the ilmenite concentrate.

The excess potassium is observed in both digestion products, as the potassium reacts with $FeTiO_3$ as the potassium titanates ($K_4Ti_3O_8$, $K_2Ti_8O_{17}$, $K_2Ti_6O_{13}$) during alkali digestion. And the content of silicon in the digestion product performed by the steel beaker decreases, but that in the digestion product carried out by the glass beaker significantly increases. It may be considered as too much excess silicon in digestion products, which is performed by glass beaker, is caused by the corrosion and decomposition of glass beaker due to the reactions of glass with KOH at high temperature and long period of digestion time.

The extraction efficiencies of Ti operated with a steel beaker are much more preferable compared to those operated with a glass beaker, and the steel beaker has more corrosion resistance and a lack of interference from Si.

Table 4. Metals Extraction Efficiencies in Different Containers with Relevant Optimum Digestion Times and Ilmenite to Alkali Weight Ratio

Elements	Content in Ilmenite Concentrate	Content in Digestion Product, 240 min, 1:5, (Glass Beaker)	Content in Digestion Product, 120 min, 1:5, (Steel Beaker)
Ti	6.036 g	4.206 g	5.926 g
Fe	**4.466 g**	**2.971 g**	****4.551 g**
Si	**0.472 g**	***2.610 g**	**0.202 g**
K	0.007 g	2.247 g	2.273 g

*Containing Si Content from Glass Beaker

**Containing Fe Content from Steel Beaker

Mineralogical Analysis of Synthesised TiO_2 and Calculation of Nanoscale

The XRD results shown in Figure 9 (a) and (b) indicate that the resultant TiO_2 calcined at 500 ℃ is in a form of anatase and calcined at 900 ℃ is in a form of rutile. It is observed that the formation of anatase and rutile phase TiO_2 is mainly dependent on the calcination temperature.

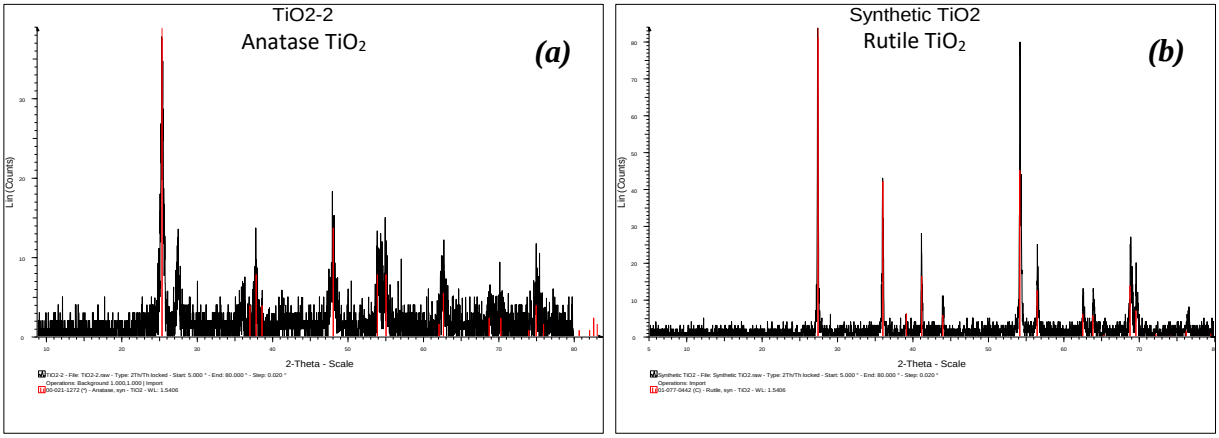

Figure 9. XRD spectra of synthesised *(a)* anatase and *(b)* rutile TiO_2

The X-ray diffraction peaks of resultant anatase TiO_2 NPs appear at 2θ values of 25.240°, 47.941°, and 54.958° (JCPDS No. 21-1272). The 2θ value of 25.240° is the highest peak for the resultant anatase TiO_2 NPs. And the X-ray diffraction peaks of resultant rutile TiO_2 NPs appear at 2θ values of 27.334°, 35.955°, and 54.216° (JCPDS No. 77-0442). The 2θ value of 27.334° is the highest peak for the resultant rutile TiO_2 NPs. The resultant anatase and rutile TiO_2 NPs are crystalline and the particle sizes are calculated by using the following Debye-Scherrer equation;

$$D = \frac{K\lambda}{\beta\, Cos\theta} \qquad (3)$$

Where D is the crystallite size, K is the Scherrer constant (0.941), λ is the wavelength of the radiation, and β is the full width at half maximum height (FWHM) of the peak. The average particle sizes calculated by the Scherrer formula for the resultant anatase and rutile TiO_2 NPs are ~46 nm and ~61 nm.

Elemental Analysis of Synthesised TiO_2 NPs

According to the ED-XRF analysis of the resultant TiO_2, TiO_2 purity has progressed up to ~94.19 % by EDTA: Fe molar ratio of 5:1. It means that Ti is recovered from ilmenite concentrate up to ~93 % and Fe is removed about ~97.28 %. The iron removal process is also performed with the EDTA/Fe molar ratio of 8:1 and 10:1, but the titanium content is decreased and iron content is increased with the increase of EDTA: Fe molar ratio. It can be assumed that under the condition of many excess EDTA: Fe stoichiometric ratios, Ti ions may also be chelated by EDTA.

The appearance of resultant anatase TiO_2 before and after calcination is compared in figures 10 (a) and (b). After the calcination process, the appearances of the resultant TiO_2 products do not significantly change and results in white and off-white in colour.

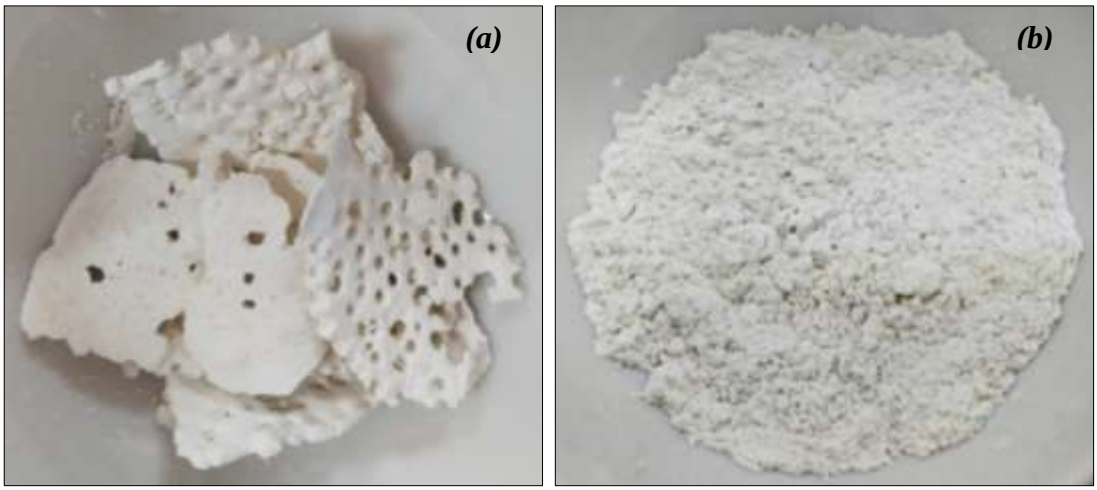

Figure 10. Appearances of *(a)* dried ($TiO_2.xH_2O$) and *(b)* calcined product (TiO_2 anatase)

The filtrate obtained as a by-product from iron removal process contains sodium, potassium, chlorine, sulfur, iron, manganese, aluminium, titanium, silicon, calcium and zinc. Some of them can be related to the stability constant of metal ion complexes with EDTA. The stability constant of the Fe(III)-EDTA complex is 25.1, and that of TiO(II)-EDTA is 17.3, and this shows that Fe(III)-EDTA is more stable. This difference in stability constants can be used for selective separation of the products. However, some of the titanium remained by chelation does not precipitate and this leads to reducing the overall efficiency of the process.

Surface Morphological Analysis of Synthesised TiO_2 NPs

The corresponding SEM micrographs of TiO_2 anatase and rutile are shown in Figures 11 (a) and (b). It shows that the anatase phase TiO_2 has an irregular shape and large size distribution, and the rutile phase TiO_2 has round shape and exhibits relatively better distribution compared to anatase TiO_2.

The non-uniform anatase phase TiO_2 crystallises plate-like and rock-like structures with an average particle length of ~16 µm and with an average particle width of ~10 µm, and rutile crystallises spherical structure with a mean diameter of 1µm.

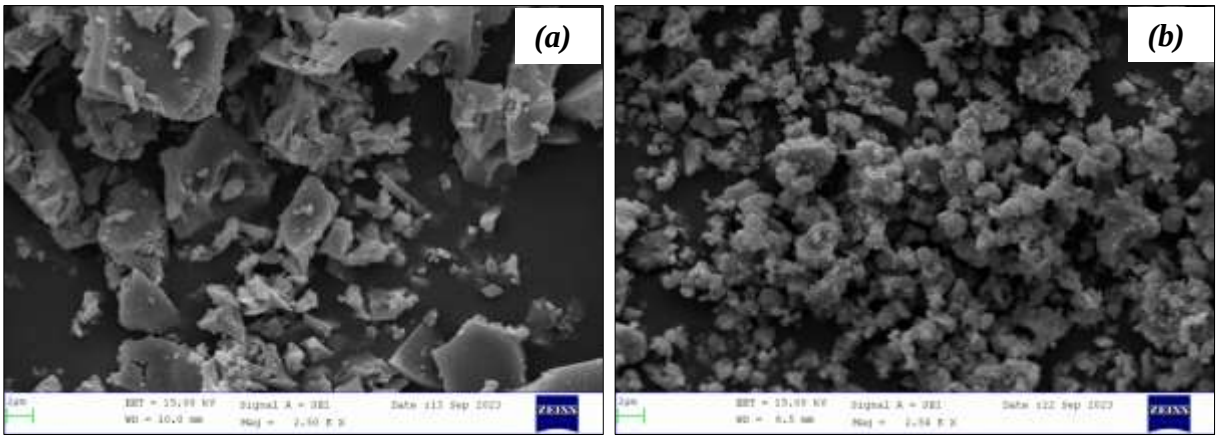

Figure 11. SEM micrographs of synthesised *(a)* anatase and *(b)* rutile TiO_2

The amorphous structure of TiO2 becomes crystallite through calcination. Concurrent with the crystalline structure change, the anatase phase undergoes a transition into the rutile phase. Energy balance as a function of crystallite size is intimately linked to this change in

crystalline structure. Because the anatase phase is unstable at high temperatures, large particles are formed when the anatase particles stick together at the higher calcination temperature. From the amorphous precursor, the anatase phase is formed as the temperature rises from 350 to 650 °C. From 650 to 1000 °C, the anatase TiO2 changes into the rutile phase TiO_2.

Conclusion

Moemeik Myitsone HMS contains Ti 11.1 % therefore it is profitable for this research work. Ti is enriched to 30.18 % in the ilmenite concentrate by means of physical beneficiation.

The major phases in all of the digestion products are roughly amorphous, and discernible peaks are not found in the XRD spectra. The majorities of the residue are composed of $FeTiO_3$, Fe_2O_3, and SiO_2 as in the raw sample. The residual particles are grouped into spherical aggregates, and these aggregates are as big as 200 μm on average. Longer digestion times at high temperatures cause the masking on ilmenite particles and no longer able to react with KOH solution.

The extraction efficiencies of Ti operated with steel beaker for all of the variations of digestion parameters are much preferable compared to those operated with glass beaker, furthermore steel beaker has more corrosion resistant and lack of interference from Si.

The TiO_2 NPs are white and off-white in colour and purity is ~94.2 %. Ti is recovered at about ~93 % and Fe is removed more than 97 %. And the average particle sizes for the resultant anatase and rutile TiO_2 NPs are ~46 nm and ~61 nm. Since, the anatase phase is unstable at high temperatures; large particles are formed when the anatase particles stick together at the higher calcination temperature. According to the SEM images, anatase phase TiO_2 crystallises in plate-like and rock-like structure, and rutile crystallises in spherical structures.

The filtrate obtained as a by-product from the iron removal process has beneficial constituents such as Fe(III)-EDTA complex, potassium, sulfur, manganese, and chloride ions which are essential elements for effective growth of plants, therefore it can be used as fertiliser in agricultural fields. Accordingly, this matter can make this process more attractive and mitigate the economic criteria and environmental effects. In addition, it is possible to recycle the consumed EDTA via different methods.

Accordingly, the optimum digestion parameters for the alkali digestion process are an alkali concentration of 72 %, ilmenite to alkali wt. ratio of 1:5 with a steel beaker at 220 ℃ for 120 min. EDTA/Fe molar ratio 5:1 is suitable for the iron removal process. And the by-products containing Fe-EDTA can be used for supplying micronutrients to crops.

Acknowledgements

The current study was carried out at the Laboratory of Faculty of Chemistry, D.S.A. The authors gratefully acknowledge to Commandant and Rector of D.S.A for the permission and encouragement for this research work. Moreover, authors express their great thanks to Dean of the Faculty of Chemistry for his supervision to this work.

References

Ajamaluddin Malik et al., (2021) "Impact of Metal Nanoparticles on the Structure and Function of Metabolic Enzymes", International Journal of Biological Macromolecules 188 576–585.

Bradley S. Van Gosen et al., (2016) "Coastal Deposits of Heavy Mineral Sands; Global Significance and US Resources" Mining Engineering, October.

Iqbal Firdaus et al., (2021) "Synthesis and Characterization of TiO2 from Lampung's Iron Sand using Leaching Method with Temperature Variation", JFA (JURNAL FISIKA DAN APLIKASINYA) VOLUME 17, NUMBER 2, JUNE.

Seman N et al., (2022) "Preparation Method of Titanium Dioxide Nanoparticles and Its Application: An Update", IOP Conf. Series: Earth and Environmental Science 1091, 012064.

Shilpy Bhullar et al., (2021) "Rapid Green-synthesis of TiO2 Nanoparticles for Therapeutic Applications". RSC Adv., 11(48), 30343–30352.